

# Experimental investigation of the convective heat transfer characteristics of TiO<sub>2</sub>/distilled water nanofluids under constant heat flux boundary condition

Munish Gupta · Rajesh Kumar · Neeti Arora ·  
Sandeep Kumar · Neeraj Dilbagi

Received: 23 July 2014 / Accepted: 8 October 2014 / Published online: 19 October 2014  
© The Brazilian Society of Mechanical Sciences and Engineering 2014

**Abstract** This paper presents the experimental investigation of convective heat transfer characteristics of nanofluid containing TiO<sub>2</sub> and distilled water inside a copper tube under laminar flow condition. Nanofluids with different particle weight concentration of 0.05, 0.1, 0.3 and 0.5 wt % are used in the present investigation. The effects of nanoparticles weight concentration on heat transfer coefficient and Nusselt number in the velocity range (0.1659–0.2322 m/s) under constant heat flux boundary conditions have been studied. The constant velocity criterion has been taken in order to get an accurate picture of convective heat transfer performance of nanofluids relative to base fluid. It is observed that the heat transfer coefficient increases with the increase in the particle weight concentration and flow velocity. Results revealed that the heat transfer coefficient increases from 29.93 to 50.11 % by increasing the concentration from 0.1 to 0.3 wt % as compared to distilled water in the given velocity range. The nanofluids show a decrease in heat transfer at higher concentration (0.5 wt %).

**Keywords** Nanofluids · Convective heat transfer · Laminar flow · Constant heat flux

## Abbreviation

### List of Symbols

$c_p$	Specific heat (J/Kg K)
$D$	Diameter of copper tube (m)
$h$	Heat transfer coefficient (W/m <sup>2</sup> K)
$k$	Thermal conductivity (W/m K)
$L$	Tube length (m)
$\dot{m}$	Mass flow rate (kg/s)
$Nu$	Nusselt number
$q''$	Heat flux (W/m <sup>2</sup> )
$Pr$	Prandtl number
$Re$	Reynolds number
$T$	Temperature (°C)
$x$	Distance from the pipe inlet (m)
$A$	Heat transfer area (m <sup>2</sup> )
$I$	Current (A)
$Q$	Heat transfer (W)
$U$	Velocity (m/s)
$V$	Voltage (V)
$\rho$	Density (kg/m <sup>3</sup> )
$\phi$	Volume fraction
$\mu$	Dynamic viscosity (Pa s)
$\Delta P$	Pressure drop (Pa)

## Subscripts

f	Base fluid
i	Inlet
m	Bulk
nf	Nanofluids
bf	Base fluid
p	Particle
s	Surface
x	Local

Technical Editor: Francisco Ricardo Cunha.

M. Gupta · R. Kumar (✉) · N. Arora  
Department of Mechanical Engineering, Guru  
Jambheshwar University of Science and Technology,  
Hisar 125001, Haryana, India  
e-mail: rajeshkumar007gu@gmail.com

S. Kumar · N. Dilbagi  
Department of Bio and Nano Technology, Guru  
Jambheshwar University of Science and Technology,  
Hisar 125001, Haryana, India

## 1 Introduction

Fluids play a vital role in various heat transfer devices used in industry such as electronics, transportation, chemical processes, power plant, air-conditioning, food processing, nuclear reactors etc. for cooling and heating purposes. The conventional heat transfer fluids like water, ethylene glycol, propylene glycol, oil, gear oil and paraffin are mostly used for this purpose. They have poor thermal properties which restrict the performance of the heat transfer devices. Many active and passive techniques are available to improve the thermal performance of conventional fluids [1, 2]. Solid materials have better thermal properties than fluids. Many studies have been carried out on thermal properties of suspension of these solid particles in conventional heat transfer fluids. The dispersion of millimeter or micrometer size solid particles to the base fluid results in modification of thermophysical properties of the base fluids that ultimately leads to heat transfer enhancement [3]. However, the application of these fluids is limited due to some serious problem i.e., the poor stability of suspensions, clogging, erosion of pipelines and pressure drop. To overcome these problems nano-sized particles dispersed in the base fluid known as nanofluids, were firstly introduced by Choi [4]. These novel fluids reflected improved heat transfer properties because they have small size and large specific areas. A wide range of experimental and theoretical studies has been carried out on the internal forced convective heat transfer of nanofluids with different boundary conditions in laminar [5] and turbulent [6, 7] flows. Rayatzadeh et al. [8] investigated the convective heat transfer and pressure drop of  $\text{TiO}_2$ /distilled water nanofluids under constant heat flux boundary condition. This experiment has been performed with and without a continuous induced ultrasonic field. The experiment was performed in the laminar flow regime in 0.1–0.25 % volume concentrations. It was observed that the nanofluids show enhancement of heat transfer as compared to base fluid. The Nusselt number indicated decreases in heat transfer at higher concentration, i.e. 0.25 % volume concentration without sonication. 5 % increment was also observed in Nusselt number with higher concentration using continuous ultrasonic waves compared with results obtained without any sonication. Sahin et al. [9] studied the convective heat transfer and pressure drop characteristics of  $\text{Al}_2\text{O}_3$ -water nanofluid for turbulent flow regime inside a circular tube under constant heat flux boundary condition. The experiments were performed using 0.5–4 % volume concentration in the Reynolds range 4,000–20,000. The results show that up to 1 % concentration the Nusselt number increased with both increase in Reynolds number and volume concentration. The concentrations higher than 1 vol. % were not suitable for heat transfer. The highest heat transfer enhancement was achieved at  $Re = 8000$  and 0.5 % volume concentration.

Esmailzadeh et al. [10] investigated  $\gamma$ - $\text{Al}_2\text{O}_3$ /water nanofluid under a laminar flow regime having constant heat flux boundary condition. The results show that the convective heat transfer coefficient increases with the increase in particle volume concentration. The enhancement of heat transfer coefficient was found to be 6.8 % at 0.5 % volume concentration and it increased to 19.1 % with 1 % volume concentration as compared to the base fluid. A similar study was conducted by Wen and Ding [11] for  $\text{Al}_2\text{O}_3$ /water nanofluid in the entrance region under laminar flow conditions. It was observed that the use of specified nanoparticles as the dispersed phase in water improve the convective heat transfer, and the enhancement increased with Reynolds number, as well as particle volume concentration.

He et al. [12] studied the heat transfer and flow behavior of aqueous suspensions of  $\text{TiO}_2$  nanoparticles (nanofluids). The nanofluids flowing upward through a vertical pipe. It was observed that the heat transfer depends on particles concentration and particle size, it increases with increasing particle concentration and also decreasing particle size. The viscosity increased with increasing agglomerated particle size and particle concentration. The convective heat transfer coefficient increased with nanoparticle concentration in both the laminar and turbulent flow regimes with a given Reynolds number. Further, a study of convective heat transfer and pressure drop of an aqueous solution of spherical  $\text{TiO}_2$  nanoparticle (15 nm) through a uniformly heated horizontal circular tube in the turbulent flow regime containing 0.1, 0.5, 1.0, 1.5 and 2.0 % volume concentrations of nanoparticles was performed by Kayhani et al. [13]. Results indicated that heat transfer coefficients increased with increasing volume fraction of nanoparticles in base fluid. No change in heat transfer coefficient was observed with varying the Reynolds number in the given range. The enhancement of Nusselt number was found to be 8 % at 2.0 % nanoparticle volume fraction at  $Re = 11,800$ . Wang et al. [14] investigated carbon nanotubes (CNT) in a horizontal circular tube under constant heat flux boundary condition. The enhancement of heat transfer coefficient was found to be 70 % at 0.05 % volume concentration and it increased to 190 % with 0.24 % volume concentration as compared to the base fluid, at a Reynolds number of about 120.

The motivation behind the present study is that very less work is reported in the literature on the convective heat transfer using  $\text{TiO}_2$  nanofluids. Further, there are contradictions in stating studies on the convective heat transfer using nanofluids because of varying conditions adopted by different research groups [15–19]. The  $\text{TiO}_2$  nanoparticles are safe materials as these are reported to be used in cosmetics and are easily obtained at large scale and have excellent stability [20, 21]. This paper presents the effect of nanoparticles volume fraction in the range of 0.05–0.5wt % of the heat transfer of  $\text{TiO}_2$ -distilled water nanofluid in the

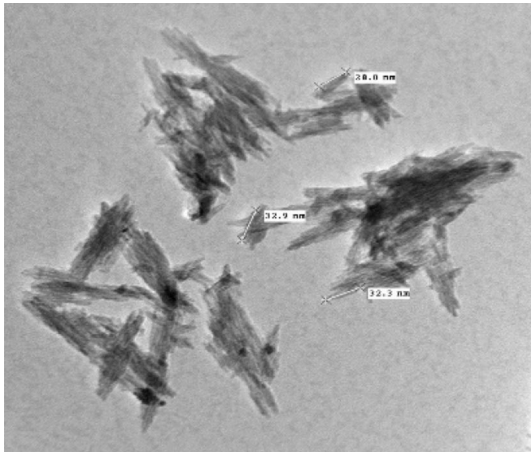


**Fig. 1** TEM images of TiO<sub>2</sub> nanoparticles

Reynolds range of 1,663–2,488 under constant heat flux boundary conditions. Further a heat transfer correlation based on the experimental results is developed.

## 2 Preparation of nanofluid

In the present study, TiO<sub>2</sub> nanoparticles purchased from Nanostructured and Amorphous Materials, USA along with distilled water as base fluid are taken. The transmission electron microscopy (TEM) images of TiO<sub>2</sub> nanoparticle are shown in Fig. 1. It can be seen from TEM images that the majority of nanoparticles is in the form of large agglomerates and appears in the form of rods in morphology. The size of these nanoparticles is in the range of 30–50 nm. Two-step method was used to make uniform and stable nanofluids. Nanofluids were prepared by dispersing 0.05, 0.1, 0.3 and 0.5 wt % of the TiO<sub>2</sub> nanoparticles in the distilled water. The mixture was sonicated using ultrasonic vibrator (POWERSONIC 410, Hwashin Technology, Korea) generating ultrasonic pulses of 400 W from 6 to 8 h. The sonicator was used to make stable suspension of nanoparticles and break down the agglomeration of nanoparticles in the fluid. We did not employ any surfactant as they may have some effect on the effective thermal conductivity of nanofluids [22]. It was detected with naked eyes that the nanoparticles were dispersed homogeneously in a base fluid for 48 h and the whole sedimentation happened after three weeks. The dispersed TiO<sub>2</sub> nanoparticles in the water base fluid are represented in Fig. 2.

## 3 Experimental set up

The apparatus used in this experiment involves a peristaltic pump, test section, a reservoir tank, cooling unit, D.C.

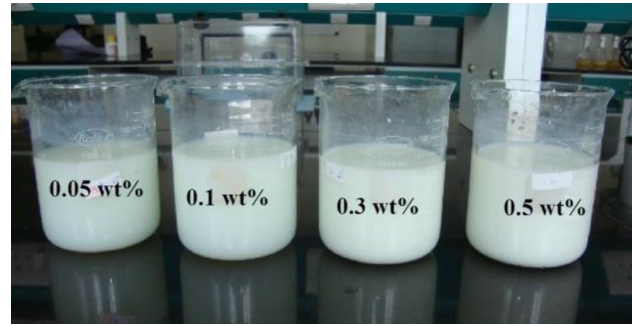


**Fig. 2** TiO<sub>2</sub> nanofluid at various particle concentrations

heating section and thermocouples. The test section consists of a copper pipe of 1.05 m length by 8 mm (I.D.) inner diameter and 10 mm outer diameter (O.D.). The test section is wrapped with sun mica to isolate it electrically.

Thereafter, electrical SWG Nichrome heating wire having a high melting point of about 1,400 °C is enfolded over it. Over the electrical winding, thick insulation consisting of glass wool is provided to prevent the radial heat loss. This heated nichrome wire is connected to a DC supply which is controlled by variac transformer (range 0–240 V). The copper tube test section has ten calibrated J-type thermocouples with 0.1 °C resolution placed at equal distance in order to measure the wall surface temperature. Two thermocouples are mounted into the flow at the inlet and outlet of the test section for measuring the temperature of the nanofluids. The flow rates were calculated by collecting the fixed volume of fluid with the help of a precise measuring jar (1,000 ml) with 10 ml resolution and measuring the time with stop watch having 0.1 s resolution. The schematic of the experimental setup is shown in Fig. 3.

The nanofluids with different weight fraction of 0.05, 0.1, 0.3 and 0.5 % TiO<sub>2</sub>/distilled water were taken in the test section with the help of peristaltic pump and uniformly heated by nichrome wire. After passing through the test section, nanofluids enters the cooling section and the nanofluids outlet temperature reduces significantly. Finally, the flow is measured in the flow measuring section. During experimental runs, inlet and outlet temperature of nanofluids and the wall temperature at different position were measured. Each measurement was repeated at least five times.

## 4 Data reduction

Prior to the study of the convective heat transfer performance of the nanofluids, the thermophysical properties of nanofluid must be evaluated. These thermophysical properties are computed using the Eqs. (1)–(4). The density of

**Fig. 3** a Schematic view of the experimental setup b experimental setup for investigation the convective heat transfer characteristics of nanofluids

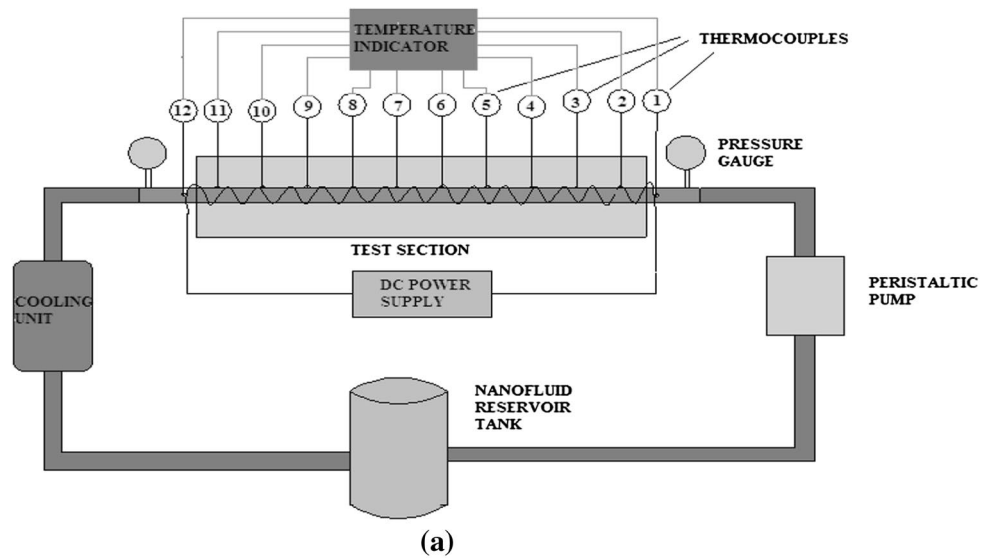


**Table 1** Thermophysical properties of base fluid and TiO<sub>2</sub> nanoparticles at 30 °C

Substance/ nanoparticles	Density (kg/m <sup>3</sup> )	Thermal conductivity (W/m K)	Specific heat (kJ/kg K)	Viscosity (kg/ms)
Distilled water	1,000	0.62	4.187	0.000798
TiO <sub>2</sub> [27]	4,260	11.7	6.89	–

nanofluids is estimated by Pak and Cho equation [23]. The specific heat of nanofluids is estimated by the equation given by Xuan and Roetzel [24].

$$\rho_{nf} = \phi\rho_p + (1 - \phi)\rho_{bf} \tag{1}$$

$$(\rho Cp)_{nf} = \phi(\rho Cp)_p + (1 - \phi)(\rho Cp)_{bf} \tag{2}$$

The well-known Einstein’s equation for calculating viscosity, applied to spherical particles having volume fractions less than 5.0 vol. %, suggested by Drew and Passman

[25] has been used to evaluate the viscosity of the nanofluid as follows

$$\mu_{nf} = (1 + 2.5\phi)\mu_{bf} \tag{3}$$

The thermal conductivity of the nanofluids is calculated from the model presented by Maxwell [26].

$$k_{nf} = \frac{2k_{bf} + k_p + 2\phi(k_p - k_{bf})}{2k_{bf} + k_p - \phi(k_p - k_{bf})}k_{bf} \tag{4}$$

The thermophysical properties of nanoparticles (TiO<sub>2</sub>) and base fluid are used in the present study are given in Table 1. The thermophysical properties of nanofluids at different concentration using above equation are presented in Table 2. By assuming the test section to be well insulated and the neglecting heat loss, heat flow is equal to the power input.

Heat supplied to the test section is calculated as follows:

$$Q_1 = VI \tag{5}$$

Heat absorbed by the nanofluid is calculated by:

**Table 2** Thermophysical properties of nanofluids at different concentrations

Nanofluids	Wt %	Vol %	Density (kg/m <sup>3</sup> )	Thermal conductivity (W/m K)	Specific heat (kJ/kg K)	Viscosity (kg/ms)
TiO <sub>2</sub> /distilled water	0.05 wt	0.0117	1038.1	0.6388	4.3168	0.00082134
TiO <sub>2</sub> /distilled water	0.1 wt	0.0234	1076.3	0.6580	4.4373	0.00084468
TiO <sub>2</sub> /distilled water	0.3 wt%	0.0703	1229.2	0.7391	4.8456	0.00093825
TiO <sub>2</sub> /distilled water	0.5 wt%	0.117	1381.4	0.8271	5.1622	0.0010

$$Q_2 = mc_p(T_o - T_i) \tag{6}$$

where ‘T<sub>o</sub>’ and ‘T<sub>i</sub>’ are the outlet and inlet temperatures of nanofluids in the test section respectively.

Heat flux is calculated as follows:

$$q'' = \frac{Q}{\pi DL} \tag{7}$$

where ‘D’ is the copper tube inner diameter, ‘L’ is the length of the tube and ‘Q’ is the heat transfer rate which obtains from the Eq. (8).

$$Q = \frac{Q_1 + Q_2}{2} \tag{8}$$

The convective heat transfer coefficient ‘h’ is given as follows:

$$h = \frac{q''}{T_s - T_m} \tag{9}$$

where,  $T_m = \frac{T_{in} + T_{out}}{2}$  (10)

and  $T_s = \frac{\left(\sum_{i=2}^{11} T_i\right)}{10}$  (11)

‘T<sub>m</sub>’ and ‘T<sub>s</sub>’ are bulk temperature and mean surface temperature respectively. The Nusselt number is calculated as follows:

$$Nu = \frac{hD}{k_{nf}} \tag{12}$$

The local heat transfer coefficient and Nusselt number will be determined by replacing ‘h’ by h(x) and ‘Nu’ by Nu(x).

Where  $h(x) = \frac{q''}{T_s(x) - T_m(x)}$  (13)

$$Nu(x) = \frac{h(x) \times D}{k_{nf}} \tag{14}$$

T<sub>m</sub>(x) can be calculated from:

$$T_m(x) = T_{m,i} + \frac{q''P}{m \times C_p}x \tag{15}$$

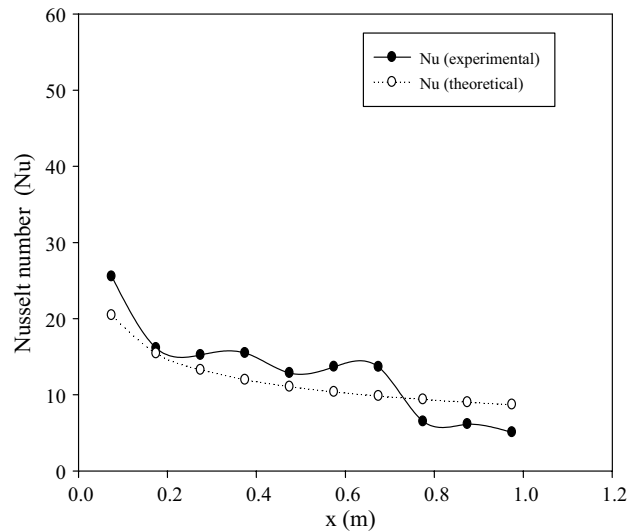


**Fig. 4** Comparison of the measured local Nusselt number with the empirical equation for distilled water under the constant heat flux condition for the laminar flow regime

where ‘P’ is the perimeter and ‘m’ is the mass flow rate.

## 5 Result and discussion

### 5.1 Validation of the experimental setup

In order to access the consistency and correctness of the experimental setup, the experiments were conducted using distilled water as the working fluid in the plain copper tube under laminar flow conditions before obtaining these results for nanofluids. The Nusselt number of distilled water was measured in several runs to obtain repeatability of the experiment. Figure 4 shows the comparison of experimental results of distilled water with Shah equation [28] for Nusselt number along the axial direction for fixed Reynolds number (In the present study it was kept 1995) for laminar flow under constant heat flux.

$$Nu(x) = \begin{cases} 1.953(\text{Re} \cdot \text{Pr} \cdot \frac{D}{x})^{1/3} & (\text{Re} \cdot \text{Pr} \cdot \frac{D}{x}) \geq 33.3 \\ 4.364 + 0.0722\text{Re} \cdot \text{Pr} \cdot \frac{D}{x} & (\text{Re} \cdot \text{Pr} \cdot \frac{D}{x}) < 33.3 \end{cases} \tag{16}$$



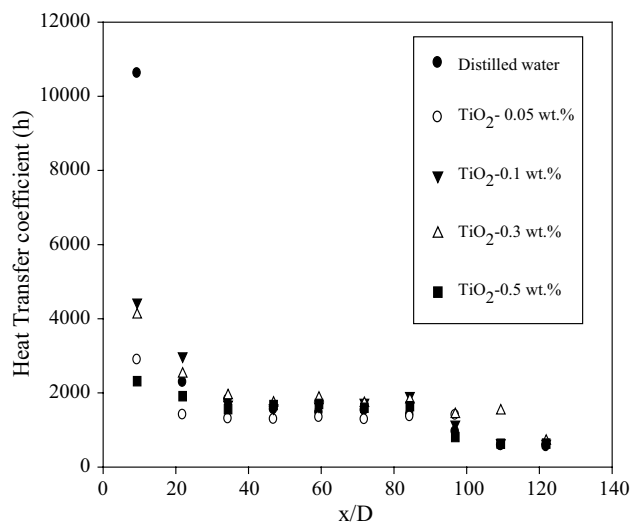


**Fig. 5** Comparison of local heat transfer coefficient versus non-dimensional axial distance of nanofluids and base fluid

It can be seen from Fig. 4 that there is a good agreement between the experimental results and the calculated values for distilled water.

## 5.2 Heat transfer

In this experimental work,  $\text{TiO}_2$ -distilled water nanofluid with loading of 0.05, 0.1, 0.3 and 0.5 wt % were used. All the experiments have been performed in the Reynolds number range of 1,663–2,488. Figures 5 and 6 shows the comparison of local heat transfer coefficient and Nusselt number along non-dimensional axial distance for the various weight concentrations of nanofluids and distilled water. The results show that the maximum enhancement rate is attained at the inlet of the test section and this rate of enhancement shrinks along the axial distance from the inlet of the test section. This fact is based on the thermal boundary layer. The thermal boundary layer is very small in the beginning of the test section and due to this reason, the thermal resistance is reduced, which leads to an increase in the heat transfer coefficient in the entry region. Moving away from the inlet of the test section, the thermal boundary layer becomes developed and due to this fact, the thermal resistance increases and the heat transfer reduces.

Earlier research groups [8, 13] have taken constant Reynolds number as the basis of comparison between the nanofluids of different concentrations and distilled water. Yu et al. [29, 30] stated that the Reynolds number is an unsuitable basis for comparing the convective heat transfer characteristics of a nanofluid in comparison with the distilled water. The constant Reynolds number comparison is suitable when we consider the same fluid. But in case of comparison of nanofluids with the base fluid the

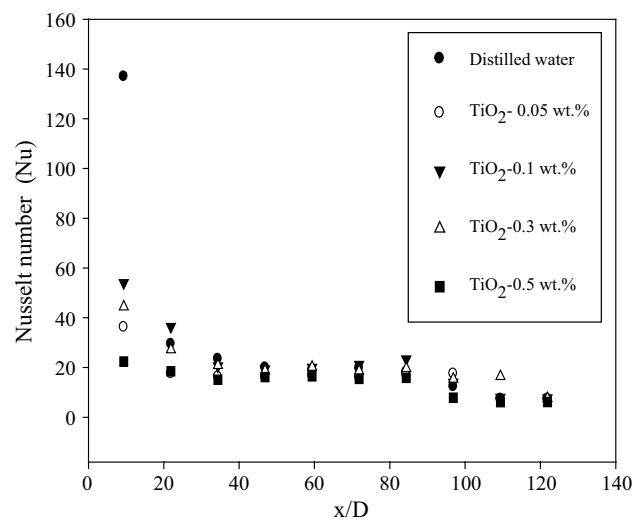


**Fig. 6** Comparison of local Nusselt number versus non-dimensional axial distance of nanofluids and base fluid

thermophysical properties of the nanofluids like density, thermal conductivity, viscosity, etc. are different from the distilled water. Hence, if we take a constant Reynolds number criteria the velocity of the nanofluid will not remain same at a fixed Reynolds number. The velocity is a function of heat transfer coefficient. Therefore, the constant Reynolds number criterion alters the physical situation and hence it is not suitable for comparing the convective heat transfer of nanofluids compared to the base fluid. If we consider the same flow velocity of nanofluids and base fluid, the flow velocity effect present in the constant Reynolds number comparison gets eliminated.

Thus, in this paper the constant velocity comparison for convective heat transfer coefficient and Nusselt number at different volume concentration is performed instead of constant Reynolds number comparison. This is done to provide the accurate picture of heat transfer performance. However, it should be noted that, for the nanofluids the viscosity is greater than the distilled water and it increases with the increase in concentration, so the pumping power would be higher for nanofluids as compared to the less viscous base liquid under the comparison of constant flow velocity. But when the flow system under consideration is designed for a certain maximum flow rate and the flow pumping power is only a fractional part of the total power consumed, the constant flow velocity comparison provides a quite precise picture of the forced single-phase convective heat transfer performance of a nanofluid relative to its base fluid [29]. At the constant velocity the pumping power difference between a nanofluid and its base fluid is quite small in many engineering applications.

The results obtained using constant velocity comparison criteria within the range (0.1659–0.2322 m/s) at various

concentrations of nanofluids are represented in Fig. 7. It can be observed that the heat transfer coefficient of the nanofluids is greater than those of the base liquid and it increases with an increase in the flow velocity. Further it also increases with the increase in the particle weight concentration. This can be attributed to the increase in effective thermal conductivity of nanofluids. Along with the enhanced thermal conductivity, the particle movement in the middle of the tube due to the brownian motion and thermophoresis, results in flattened velocity profile and increase the energy exchange in the fluid. The thermal dispersion of nanoparticles leads to steeper temperature gradient between the fluid and the wall causing significant increases in heat transfer. The augmentation of convective heat transfer coefficient were 22.56, 29.93 and 50.11 % for the 0.05, 0.1 and 0.3 wt % of TiO<sub>2</sub>-distilled water nanofluid compared to the distilled water, respectively. The highest value of heat transfer coefficient was observed at 0.3 wt %. The heat transfer coefficient value reduces from the highest to lowest from 0.3 wt % to 0.05 wt %. The percentage increase in heat transfer coefficient at 0.5 wt % was found to be less as compared to lower concentrations. The sedimentation, combining of nanoparticles at higher concentration and higher viscosities of the nanofluids may be the cause of decrease in heat transfer improvement.

The variation of the Nusselt number versus the flow velocity is presented in Fig. 8 at different weight concentrations. It can be observed that by adding nanoparticles into the base fluid increases the nusselt number. The enhancement of nusselt number were found to be 18.37, 22.42 and 25.92 % for the 0.05, 0.1 and 0.3 wt % of TiO<sub>2</sub>-distilled water nanofluid compared to the distilled water, respectively. At higher values of the particle weight concentration i.e. at 0.5 wt % reduction in nusselt number was observed as compared to lower concentrations. As stated above for heat transfer intensification, the higher effective thermal conductivity and the chaotic motion of the nanoparticles are responsible. At higher concentration i.e., 0.5 wt % the settlement, agglomeration and higher viscosity are the probable reasons of decrease in nusselt number compared to lower concentrations.

### 5.3 Figure of merit

The figure of merit is defined as the ratio of heat transfer coefficient of nanofluids to that of the base fluid [29].

$$r = \frac{h_{nf}}{h_{bf}} \quad (17)$$

Where  $h_{nf}$  is the heat transfer coefficient of nanofluid and  $h_{bf}$  is the heat transfer coefficient of the base fluid. It is used to comparing the heat transfer performance of the nanofluids and base fluid. If the value of figure of merit is

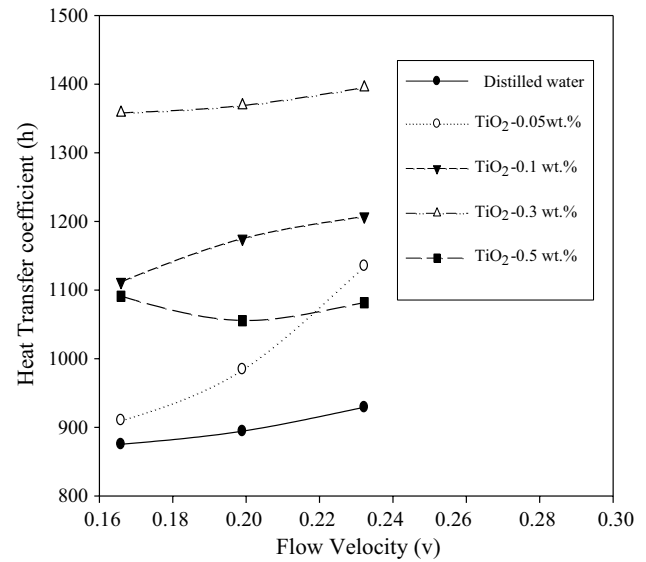


Fig. 7 Heat transfer coefficient variation of nanofluid at different flow velocity

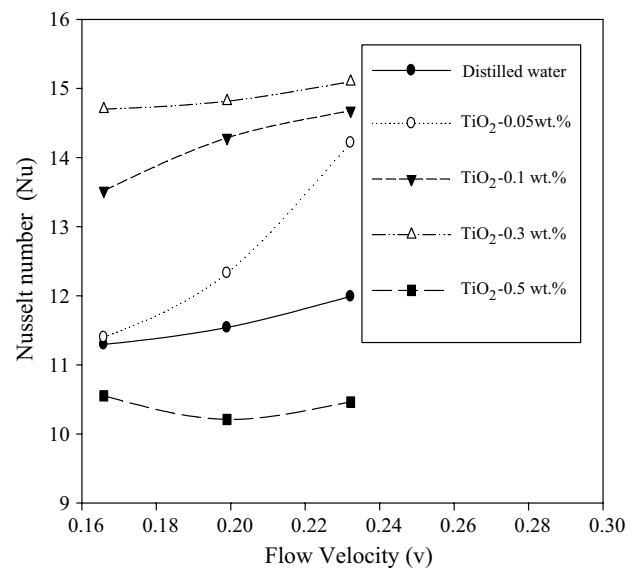
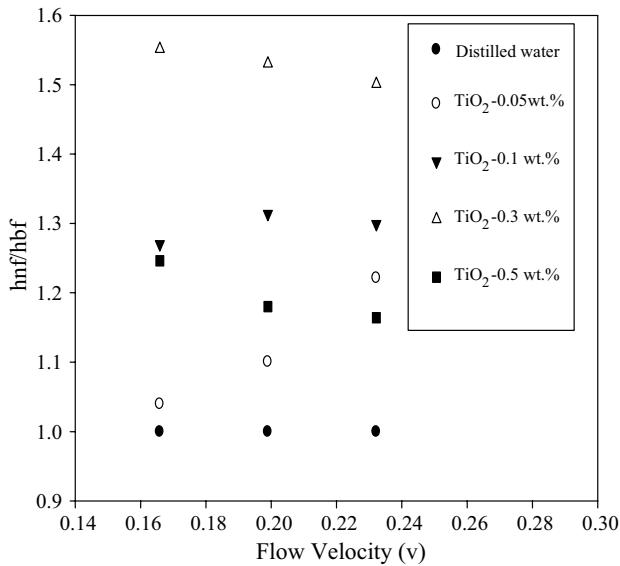


Fig. 8 Nusselt number variation of nanofluids at different flow velocity

greater than one then the nanofluid under consideration is considered beneficial for heat transfer.

The constant flow velocity comparison basis has been taken for obtaining figure of merit as a constant Reynolds number basis would be misleading as stated above. The variation of the figure of merit with flow velocity is illustrated in Fig. 9. As shown, the figure of merit improves with the increase in the flow velocity and weight concentration. Over the range of study the figure of merit for 0.03 wt % of nanofluid at



**Fig. 9** Figure of merit versus flow velocity at various weight concentrations

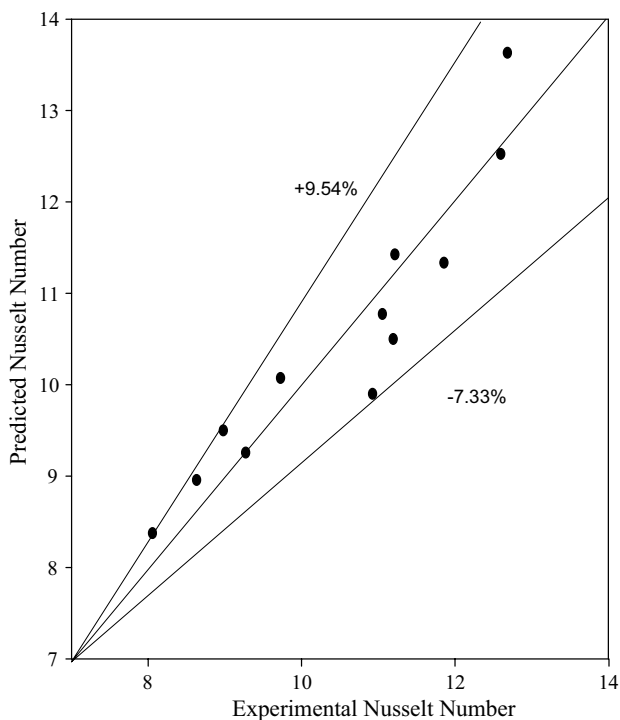


**Fig. 10** Comparison of Experimental and Predicted Nusselt number

0.1659 m/s shows the maximum value. Although the figure of merit for highest concentration 0.5 wt % taken in the present study is greater than base fluid but it is less than lower concentrations. This may be attributed to the agglomeration and sedimentation at higher concentrations as the study was conducted without addition of any surfactant. Further an experimental

**Table 3** Uncertainties of instruments and properties

Name of instrument	Variable measured	Least division in measuring instrument	Max. values measured in experiment	Uncertainty %
Thermocouple	Wall temperature, $T_w$	0.1	120	0.0833
Thermocouple	Bulk temperature $T_b$	0.1	82	0.12195
Voltage	Voltage	0.1	220	0.04545
Current	Current	0.01	10	0.1
Volume of fluid	Volume	1 ml	1,000 ml	0.1
Time taken	Time	0.01 s	60 s	0.01667
Thermal conductivity, viscosity				0.1

**Table 4** Summary of uncertainty analysis of parameters and variables

S. no.	Parameter	Uncertainties %
1	Discharge, $q$	0.101379
2	Mass flow rate, $m$	0.101379
3	Reynolds number, $Re$	0.1423997
4	Heat flux, $q''$	0.10984
5	Heat transfer coefficient, $h$	0.11644
6	Nusselt number, $Nu$	0.153487

study by Farajollahi et al. [31] showed that  $TiO_2$ /water shows fall in heat transfer at high concentration due to the dominance of the effect of increase of viscosity at higher concentrations as compared to increase of thermal conductivity.

### 5.4 Correlation for Nusselt Number

After conducting a sufficient number of experiments with nanofluids, a new correlation using multiple linear regression analysis valid for laminar flow with Reynolds number  $1663 < Re < 2433$ , for  $TiO_2$ /distilled water has been developed.

$$Nu = 0.00414.Re^{0.55}.Pr^{2.1} \tag{18}$$

The predicted values of Nusselt number are compared with the experimental values for  $TiO_2$ /distilled water nanofluids as shown in Fig. 10. It can be observed that the above correlation shows a deviation of +9.54 and -7.33 % of the experimental nusselt number.

## 6 Conclusions

An experimental study has been carried out on  $TiO_2$ /distilled water nanofluids for low concentrations under constant heat flux boundary conditions. The experiments were carried



out under laminar flow regime. The effect of flow velocity, weight concentration of nanofluids on the heat transfer coefficient and Nusselt number were investigated. The following conclusions have been obtained from the present study:

- TiO<sub>2</sub>/distilled water nanofluids display a higher heat transfer coefficient compared to the base fluids at low concentrations. The addition of small amount of TiO<sub>2</sub> nanoparticles, results in enhancement of heat transfer of nanofluids. The heat transfer coefficient also increases with increasing flow velocity within the laminar flow regime. At the flow velocity of 0.2322 m/s, for 0.3 wt % of TiO<sub>2</sub>/distilled water nanofluids, the maximum enhancement of heat transfer coefficient was 50.11 % compared to base fluid.
- It was observed that at weight concentration 0.5 wt % there was a decrease in the heat transfer coefficient as compared to lower concentrations. The sedimentation and agglomeration of nanoparticles may be the reason for the decrease in heat transfer enhancement. Further the dominance of the effect of increase of viscosity is critical in observing such behavior as compared to increase in thermal conductivity.
- The Nusselt number of nanofluid increases considerably with the increase in flow velocity. The maximum enhancement of Nusselt number was 25.92 % for the 0.3 wt % of TiO<sub>2</sub>-distilled water nanofluid compared to the distilled water.
- Using the data over the range investigated in the present experimental study, an empirical correlation is proposed to predict the Nusselt number within a deviation of +9.54 and -7.33 %.

The research work can be further extended to find out hybrid nanoparticles with enhanced heat transfer properties. An extensive work in this field can help to produce low cost nanofluids with enhanced heat transfer properties for commercialization in the heat transfer applications.

**Acknowledgments** The authors are thankful to Director, Sophisticated Analytical Instrumentation Facility (SAIF), Panjab University, Chandigarh for providing Transmission electron microscopy. The financial support for strengthening departmental facilities from funding agencies Department of Bio-technology (DBT), Department of Science and Technology (DST) and University Grants Commission (UGC), Government of India, is also greatly acknowledged.

## Appendix

### Uncertainty analysis

The systematic error analysis in the measurement of experimental analysis is estimated following the procedure given

by Beckwith et al. [32]. The uncertainties in the values estimated are summarized and presented as Tables 3, 4.

1. Discharge,  $q = \frac{\text{volume}}{\text{time}}$

$$\begin{aligned} \frac{U_q}{q} &= \sqrt{\left(\frac{U_v}{v}\right)^2 + \left(\frac{U_t}{t}\right)^2} \\ &= \sqrt{(0.1)^2 + (0.01667)^2} \\ &= 0.101379 \% \end{aligned}$$

2. Mass flow rate,  $m = \rho \times q$   
 $m = 0.101379 \%$

3. Reynold number,  $Re = \frac{4m}{\pi D\mu}$

$$\begin{aligned} \frac{U_{Re}}{Re} &= \sqrt{\left(\frac{U_m}{m}\right)^2 + \left(\frac{U_\mu}{\mu}\right)^2} \\ &= \sqrt{(0.101379)^2 + (0.1)^2} \\ &= 0.1423997 \% \end{aligned}$$

4. Heat flux,  $q'' = \frac{VI}{\pi DL}$

$$\begin{aligned} \frac{U_{q''}}{q''} &= \sqrt{\left(\frac{U_V}{V}\right)^2 + \left(\frac{U_I}{I}\right)^2} \\ &= \sqrt{(0.04545)^2 + (0.1)^2} \\ &= 0.10984 \% \end{aligned}$$

5. Heat transfer coefficient,  $h = \frac{q''}{T_w - T_b}$

$$\begin{aligned} \frac{U_h}{h} &= \sqrt{\left(\frac{U_{q''}}{q''}\right)^2 + \left(\frac{U_{T_w - T_b}}{T_w - T_b}\right)^2} \\ &= \sqrt{(0.10984)^2 + (0.0833 - 0.12195)^2} \\ &= 0.11644 \% \end{aligned}$$

6. Nusselt number,  $Nu = \frac{hD}{k}$

$$\begin{aligned} \frac{U_{Nu}}{Nu} &= \sqrt{\left(\frac{U_h}{h}\right)^2 + \left(\frac{U_k}{k}\right)^2} \\ &= \sqrt{(0.11644)^2 + (0.1)^2} \\ &= 0.153487 \% \end{aligned}$$

## References

1. Webb RL (1987) Enhancement of single-phase convective heat transfer. Wiley, NY
2. Gupta M, Kasana KS, Vasudevan R (2009) A numerical study of the effect on flow structure and heat transfer of a rectangular winglet pair in a plate fin heat exchanger. Proceedings of the Institution of Mechanical Engineers Part C. J Mech Eng Sci 223(9):2109–2115
3. Ahuja AS (2008) Augmentation of heat transport in laminar flow of polystyrene suspensions experiments and results. J Appl Phys 46(8):3408–3416

4. Choi SUS (1995) Enhancing thermal conductivity of fluids with nanoparticle, ASME FED 231–99
5. Ying Y, Zhang ZG, Grulke EA, Williams BA, Gefei WU (2005) Heat transfer properties of nanoparticle-in-fluid dispersions (nanofluids) in laminar flow. *Int J Heat Mass Transf* 48(6):1107–1116
6. Zamzamin A, Oskouie SN, Doosthoseini A, Joneidi A, Pazouki M (2011) Experimental investigation of forced convective heat transfer coefficient in nanofluids of  $Al_2O_3/EG$  and  $CuO/EG$  in a double pipe and plate heat exchangers under turbulent flow. *Exp Thermal Fluid Sci* 35:495–502
7. Sajadi AR, Kazemi MH (2011) Investigation of turbulent convective heat transfer and pressure drop of  $TiO_2$ /water nanofluid in circular tube. *Int Commun Heat Mass Transfer* 38:1474–1478
8. Rayatzadeh H, Reza M, Saffar-Avval Mansourkiaei M, Abbassi A (2013) Effects of continuous sonication on laminar convective heat transfer inside a tube using water- $TiO_2$  nanofluid. *Exp Therm Fluid Sci* 48:8–14
9. Sahin B, Gültekin GG, Manay E, Karagoz S (2013) Experimental investigation of heat transfer and pressure drop characteristics of  $Al_2O_3$ -water nanofluid. *Exp Thermal Fluid Sci* 50:21–28
10. Esmaeilzadeh E, Almohammadi H, NasiriVatan SH, Omrani AN (2013) Experimental investigation of hydrodynamics and heat transfer characteristics of  $\gamma-Al_2O_3$ /water under laminar flow inside a horizontal tube. *Int J Therm Sci* 63:31–37
11. Dongsheng W, Ding Y (2004) Experimental investigation into convective heat transfer of nanofluids at the entrance region under laminar flow conditions. *Int J Heat Mass Transf* 47(24):5181–5188
12. Yurong H, Jin Y, Chen H, Ding Y, Cang D, Lu H (2007) Heat transfer and flow behaviour of aqueous suspensions of  $TiO_2$  nanoparticles (nanofluids) flowing upward through a vertical pipe. *Int J Heat Mass Transf* 50(11):2272–2281
13. Kayhani MH, Soltanzadeh H, Heyhat MM, Nazari M, Kowsary F (2012) Experimental study of convective heat transfer and pressure drop of  $TiO_2$ /water nanofluid. *Int Commun Heat Mass Transf* 39:456–462
14. Jianli W, Zhu J, Zhang X, Chen Y (2013) Heat transfer and pressure drop of nanofluids containing carbon nanotubes in laminar flows. *Exp Thermal Fluid Sci* 44:716–721
15. Pak BC, Cho YI (1998) Hydrodynamic and heat transfer study of dispersed fluids with submicron metallic oxide particles. *Exp Heat Transfer* 11:150–170
16. Xuan YM, Li Q (2003) Investigation on convective heat transfer and flow features of nanofluids. *J. Heat transfer. ASME* 125:151–155
17. Wen DS, Ding YL (2004) Experiment investigation into convective heat transfer of nanofluids at the entrance region under laminar flow conditions. *Int J. Heat Mass Transf* 47:5181–5188
18. Ding YL, Alias H, Wen DS, Williams RA (2006) Heat transfer of aqueous suspensions of carbon nanotubes (CNT nanofluids). *Int J. Heat Mass Transf* 49:240–250
19. Yang Y, Zhong ZG, Grulke EA, Anderson WB, Wu G (2005) Heat transfer properties of nanoparticle-in-fluid dispersion (nanofluids) in laminar flow. *Int J. Heat Mass Transf* 48:1107–1116
20. Personal communication COLIPA unpublished dossier on the Safety of  $TiO_2$  nonmaterial, submitted in January 2012 to SCCS (Scientific Committee on Consumer Safety)
21. Kumar S, Bhanjana G, Kumar R, Dilbaghi N (2013) Synthesis, characterization and antimicrobial activity of nano titanium (IV) mixed ligand complex. *Mater focus* 2(6):475–481
22. Das SK, Putra N, Thiesen P, Roetzel W (2003) Temperature dependence of thermal conductivity enhancement for nanofluids. *J Heat Transf* 125:567–574
23. Pak BC, Cho YI (1998) Hydrodynamic and heat transfer study of dispersed fluids with submicron metallic oxide particles. *Exp. Heat Transf* 11:151
24. Xuan Y, Roetzel W (2000) Conceptions for heat transfer correlation of nanofluids. *Int J Heat Mass Transf* 43:3701–3707
25. Drew DA, Passman SL (1999) *Theory of multi-component fluids*. Springer, Berlin
26. Maxwell JC (1881) *A treatise on electricity and magnetism*, 2nd edn. Oxford, UK
27. Chandrasekhara RM, VasudevaRao V (2013) Experimental studies on thermal conductivity of blends of ethylene glycol-water-based  $TiO_2$  nanofluids. *Int Commun Heat Mass Transf* 46:31–36
28. Shah RK (1975) Thermal entry length solutions for the circular tube and parallel plates. In: *proceedings of 3rd National Heat and Mass Transfer Conference*, vol 1, Indian Institute of Technology, Bombay, HMT-11-75
29. Yu W, France DM, Timofeeva EV, Singh D, Routbort JL (2010) Thermophysical property-related comparison criteria for nanofluid heat transfer enhancement in turbulent flow. *Appl Phys Lett* 96:213109
30. Wenhua Yu, David MF, Timofeeva EV, Singh D, Routbort JL (2012) Comparative review of turbulent heat transfer of nanofluids. *Int J Heat Mass Transf* 55:5380–5396
31. Farajollahi B, Etemad SG, Hojjat M (2010) Heat transfer of nanofluids in a shell and tube heat exchanger. *Int J Heat Mass Transf* 53:12–17
32. Beckwith TG, Marangoni RD, Lienhard JH (1990) *Mechanical measurements*, 5th edn. Addison-Wesley Publishing Company, NY, pp 45–112